

Optimized Rule Sets for Automatic Landslide Characteristic Detection in a Highly Vegetated Forests

Biswajeet Pradhan and Mustafa Ridha Mezaal

3.1 Introduction

The rapid expansion of cities and the continuously increasing population in urban areas lead to the establishment of settlements in mountainous areas. This phenomenon has increased the impact of natural disasters, particularly landslides, in these mountainous areas. Landslides result in severe property losses, human casualties, and environmental damage. (2) Data interpretation is frequently based on the expert knowledge and experience of an analyst, as well as his or her familiarity with the area (Chen et al. 2014; Malamud et al. 2004). (3) Finally, additional errors can be introduced while translating image interpretation results into thematic maps (Malamud et al. 2004). High-resolution LiDAR-derived DEMs can depict ground surfaces and provide valuable information on the topographic features of possible landslide-affected areas that are covered by dense vegetation (McKean and Roering 2004). In addition, high-resolution DEMs can be utilized to identify landforms with a scale of a meter to a few meters and provide useful information about rocky and densely vegetated areas (Tarolli 2014; Van Westen et al. 2008). Minimal changes in terrain information can be easily detected using LiDAR data (Chen et al. 2015). In general, LiDAR data have a definite advantage because of their capability to penetrate vegetation canopies and provide valuable information on topographic conditions. This advantage makes LiDAR data different from other data sources, such as aerial photographs, in terms of detecting slope failure under dense vegetation (Pradhan et al. 2016). LiDAR data and their derivatives, such as hillshade, surface roughness, slope, and contour maps, provide significant and valuable information about active geological processes, such as landslides, which reshape the topography of an area. Overall, LiDAR data can serve as a promising tool for enhancing landslide inventory maps

(Kasai et al. 2009). However, distinguishing different types of landslides is important for studying the geomorphological development of hillsides and the mitigation of landslide hazards (Dou et al. 2015; Lin et al. 2013).

The remainder of this paper is organized as follows: The study area and data set are described in Sect. 2. The research methodology and the types of landslides, namely shallow and deep-seated landslides, are explained in detail in Sect. 3. The results are presented and discussed in Sect. 4. Finally, a brief summary, including the main findings and future directions, is presented in Sect. 5.

3.2 Types of Landslides

A landslide is the motion of the mass of debris, rocks, or a portion of the earth down a slope under the impact of gravity (Cruden and Varnes 1996; Guzzetti et al. 2012). Landslides are classified as either shallow or deep-seated, depending on the movement characteristics and landslide volume (Brunetti et al. 2009; Guzzetti et al. 2012). Shallow and deep-seated landslides differ in terms of size, volume, and damage influence (Zêzere et al. 2005). However, landslide mass volume is difficult to evaluate (Brunetti et al. 2009). Shallow landslides are typically associated with short high-intensity rainfall, whereas most large-scale deep-seated landslides result from the interaction between long-term rainfall and natural denudation processes (Zêzere et al. 2005). A landslide can demonstrate a sliding, flowing, falling, or toppling movement, but numerous landslides also exhibit a combination of two or more types of these movements either at the same time or during their lifetime (Cruden and Varnes 1996). A high-resolution DEM is necessary to study the characteristics of different types of landslides (Dou et al. 2015). Several techniques with various image sources have been utilized to distinguish landslide (Chang et al. 2012; Chen et al. 2014; Cruden and Varnes 1996; Dou et al. 2015; Korup 2006; Ma et al. 2016; Rau et al. 2012; Yu et al. 2015; Zêzere et al. 2005). Figure 3.1 shows a simple diagram

B. Pradhan (✉) · M.R. Mezaal
Department of Civil Engineering, University Putra Malaysia,
Serdang, Malaysia
e-mail: biswajeet24@gmail.com

illustrating the different landslide types. Meanwhile, Fig. 3.2 shows the general sketch of shallow and deep-seated landslides which is overlaid on contour map.

3.2.1 Deep-Seated Landslide

Deep-seated landslides are characterized by slope movements occurring on high-relief-energy hillsides; the span of this landslide type is comparable with the entire slope, but the displacements are relatively small compared with the slope itself (Goudie 2004; Kellerer-Pirklbauer et al. 2010). This type of landslides can be reactivated during intense events, and they can evolve into destructive failures. Deep-seated landslides are generally difficult to recognize in the field, especially when they happen in densely forested areas where quick revegetation occurs, such as in tropical forests. Vegetation indices are particularly helpful in recognizing deep-seated landslides (Vohora and Donoghue 2004). In general, optical images are unsuitable for analyzing this type of slope failures because they are usually covered by vegetation. To identify and map deep-seated landslides, the automation of recognition procedures and the integration of optical sensors with other remote sensing techniques have been proven to be highly effective (Delgado et al. 2011; Moine et al. 2009), and LiDAR data have been found useful (Agliardi et al. 2009). Automatic algorithms have been applied to achieve this task, such as supervised classification methods (Kasai et al. 2009) and standard signal processing techniques. Chen et al. (2015) showed that LiDAR data with 1-m resolution are sufficient for mapping

the geomorphology of forested areas and identifying deep-seated landslides.

3.2.2 Shallow Landslide

A shallow landslide is the movement of a mixture of water, soil, and debris; this landslide type starts on steep slopes during periods of intense rainfall (Bugnion et al. 2009). Thus, this landslide type is a threat to infrastructure, buildings, roads, and railways. The use of remote sensing images for shallow landslide detection is common; however, field data are necessary for verification. This concern is primarily ascribed to the swiftness and the spatial diffusion of these slope failures. Optical sensors, which can extract geomorphic features and cover a wide area, are suitable for studying shallow landslides (Gao and Maro 2010). Visual interpretation has also been proven useful for mapping this landslide type because the boundaries are frequently distinct after a shallow landslide event. Furthermore, automatic and semi-automatic classification algorithms have been tested in recent years (Heleno et al. 2015; Ma et al. 2016; Stumpf et al. 2014; Wiegand et al. 2013). The use of very-high-resolution (VHR) satellite images (e.g., GeoEye and WorldView) can provide high accuracy for detecting shallow landslides and creating databases of susceptible areas (Zizioli et al. 2014). The automated analysis of airborne laser scanning data has been used for post-event analysis, such as for mapping earthquake- or typhoon-triggered shallow landslides (Rau et al. 2012) and rainfall-induced landslides (Bai et al. 2012). Visual interpretations, such as shaded relief maps, slope

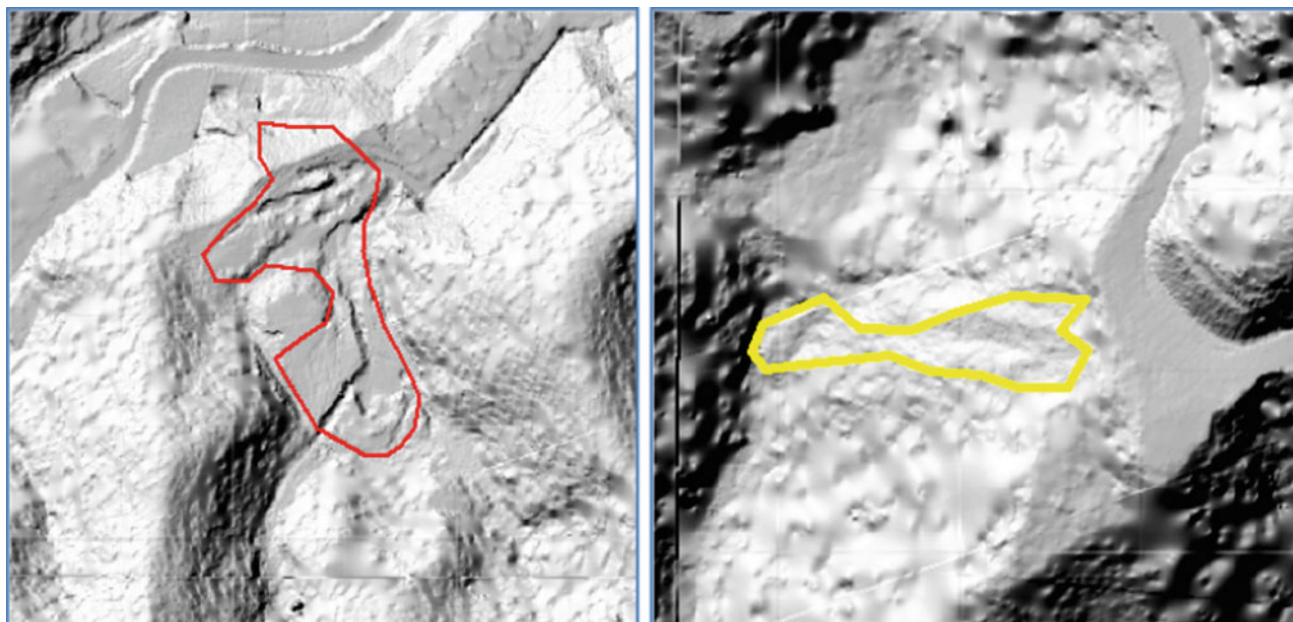
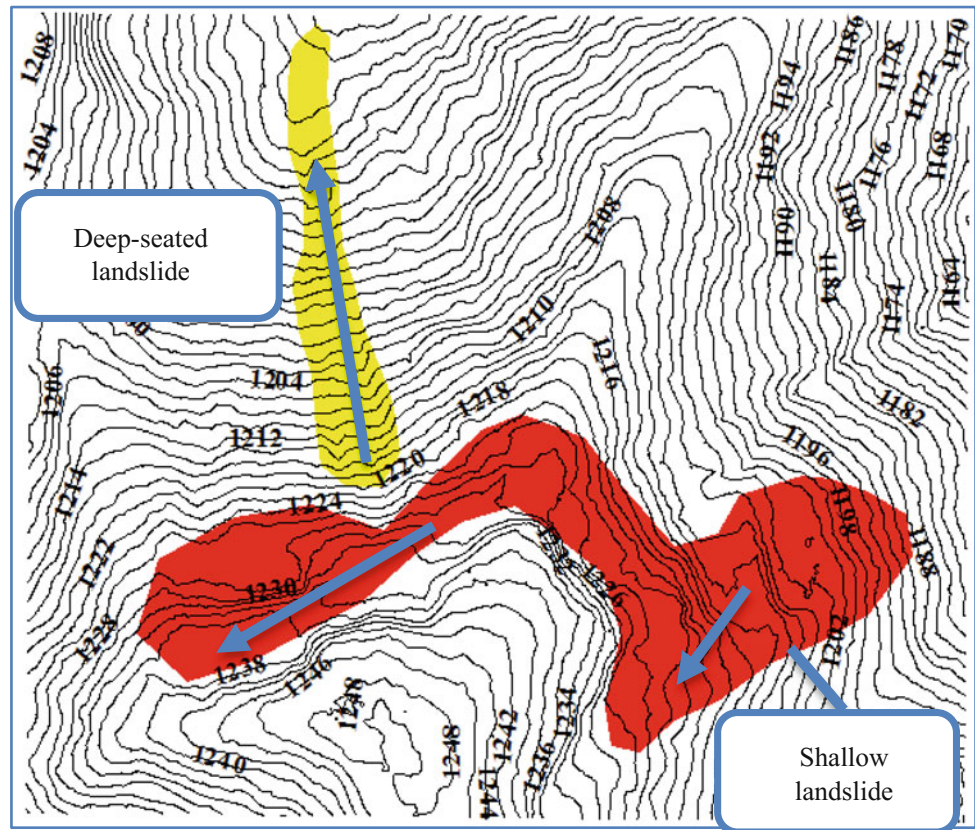


Fig. 3.1 Shallow landslide (*red polygon*) and deep-seated landslide (*yellow polygon*) in the study area

Fig. 3.2 General sketch of types of landslide



maps, and contour maps, derived from LiDAR-based DEMs were used by (Đomlija et al. 2014) to create a catalog of shallow landslides. In addition, rainfall-induced shallow landslides have been predicted using empirical rainfall thresholds or spatially distributed, physically based numerical models (Hong et al. 2015; Vennari et al. 2014). Attempts have been made to forecast this type of landslide using numerical models with both predisposing factors, e.g., landform curvature (van Asselen and Seijmonsbergen 2006) and the main triggering factor, i.e., rainfall (Segoni et al. 2009).

3.3 Study Area

The Cameron Highlands in Malaysia is a tropical rain forest area located in the latitude range $4^{\circ}22'52''$ – $4^{\circ}25'48''$ N and the longitude range $101^{\circ}22'30''$ – $101^{\circ}23'30''$ E. The Cameron Highlands is an active landslide site, and the selected subset has an aerial coverage of approximately 24.38 km^2 . The average annual rainfall in the area is 2660 mm. Its average daytime temperature is moderate ($\sim 24^{\circ}\text{C}$), whereas its nighttime temperature is 14°C . A large portion of the area (80%) is forested, and the land slopes range from 80° to flat areas (0) Fig. 3.3.

3.4 Material and Method

The multistep overall workflow of the current research is presented in Fig. 3.4. First, remote sensing data and landslide inventories were preprocessed to remove the noise and outliers from the data and prepare them for the subsequent steps. Second, a high-resolution digital elevation model (DEM) (0.5 m) was derived from the LiDAR point clouds and used to generate other LiDAR-derived products and landslide conditioning factors, such as slope, aspect, height (nDSM), hillshade, and intensity. Third, the LiDAR-derived products were combined by correcting their geometric distortions and incorporating them into a coordinate system. Then, the combined products were prepared for feature extraction using a geographic information system (GIS). Fourth, a multiresolution algorithm was used to segment the data and create image objects. In this step, the fuzzy logic supervised approach proposed by Zhang et al. (2010) was used to select the best combination of segmentation parameters (i.e., scale, shape, and compactness). Fifth, relevant attributes were selected using the correlation-based feature selection method (CFS), which ranks the attributes from the most important to the least important. Rule sets were developed by applying a decision tree (DT) algorithm using the training set of the landslide inventories and the

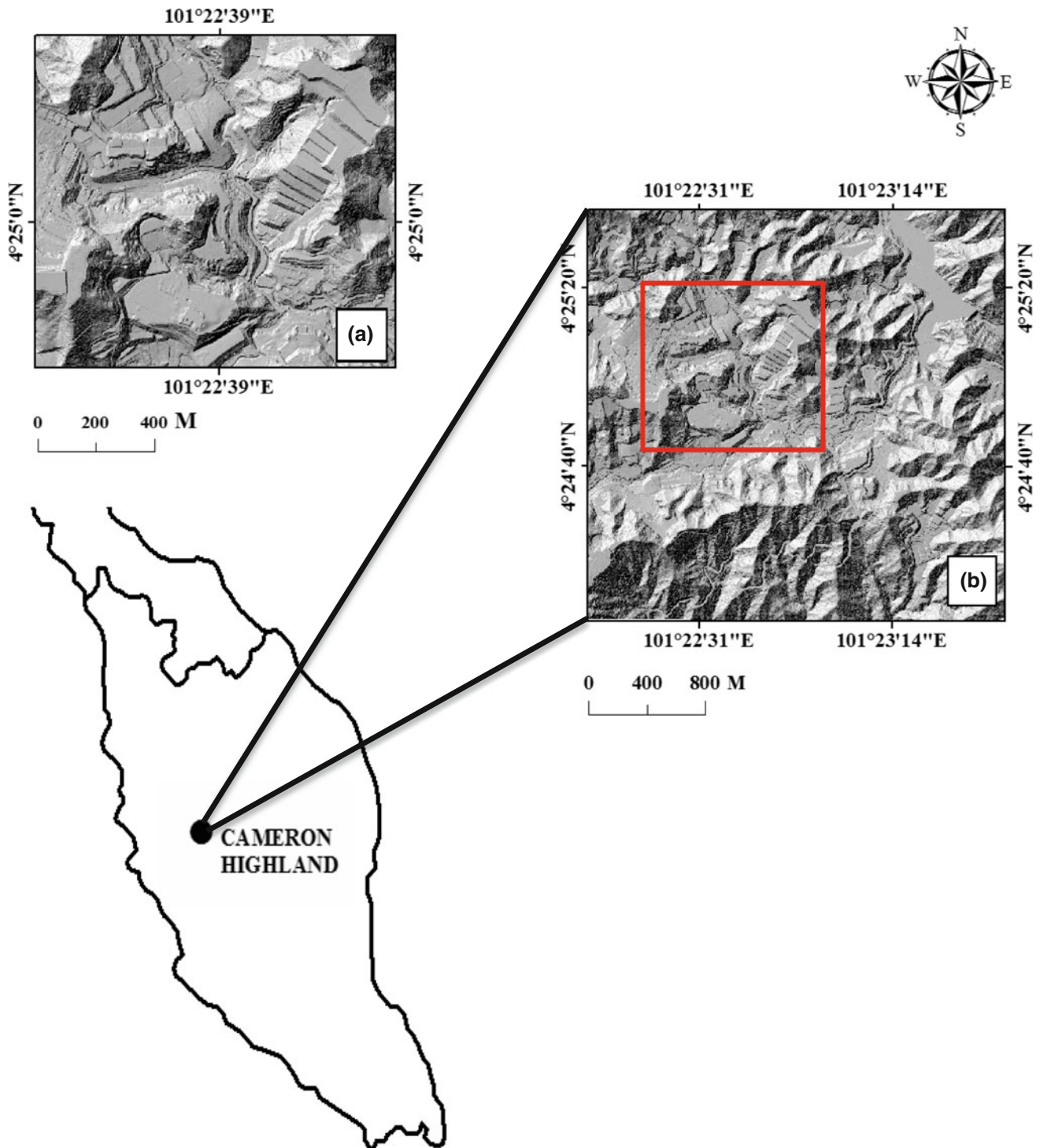
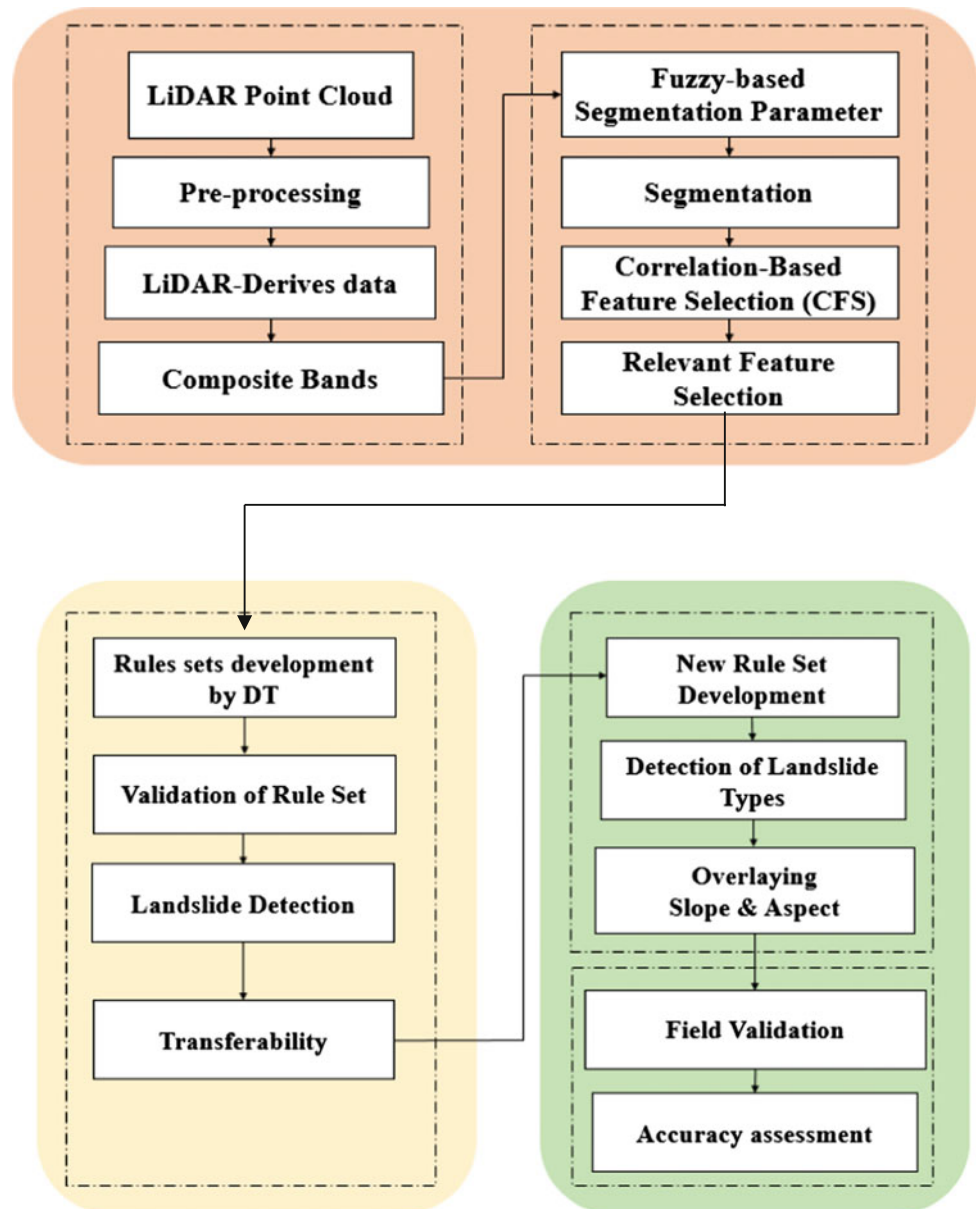


Fig. 3.3 Study area showing **a** analysis area; and **b** test area

selected relevant attributes. Rule sets were developed for extracting five land types that were enumerated as follows: (1) bare soil, (2) cut slope, (3) building, (4) vegetation, and (5) landslide. The validation of the rule sets was based on the receiver operating characteristic curves and the area under

the curve (AUC) values. Finally, the results were exported into GIS to detect the precise location and direction of the landslides by overlaying the classified segments and the hillshade on the slope and aspect data to visualize other characteristics of landslide (i.e., runoff, volume, and width).

Fig. 3.4 An overview of the method adopted in the present study



3.4.1 LiDAR Data

The LiDAR point cloud was acquired over 25 km² of the ringlet and surrounding area in Cameron Highlands at a flying height about 1510 m. The data were captured on January 15, 2015. The point density is closely 8 points per square meter with a 25,000 Hz pulse rate frequency. The absolute accuracy of the LiDAR data should meet the root-mean-square errors (RMSE) of 0.15 m in the vertical axis and 0.3 in the horizontal axis. Orthophotos were also acquired by the same system for the study area to support landslide identification and characterization.

A digital elevation model at 0.5-m spatial resolution was interpolated from LiDAR point clouds after removing the

non-ground points, with the spatial reference of GDM2000_Peninsula_RSO. The derived DEM helps in generating a number of derived layers that support landslide identification and characterization. In the current study, hillside, intensity, height (nDSM), slope, and aspect were derived from the LiDAR-based DEM Fig. 3.2, (Fig. 3.5).

3.4.2 Object-Based Image Analysis (OBIA)

An object-based approach considers the spatial, spectral, and texture attributes of the features in the classification process; thus, it is different from other classification approaches such

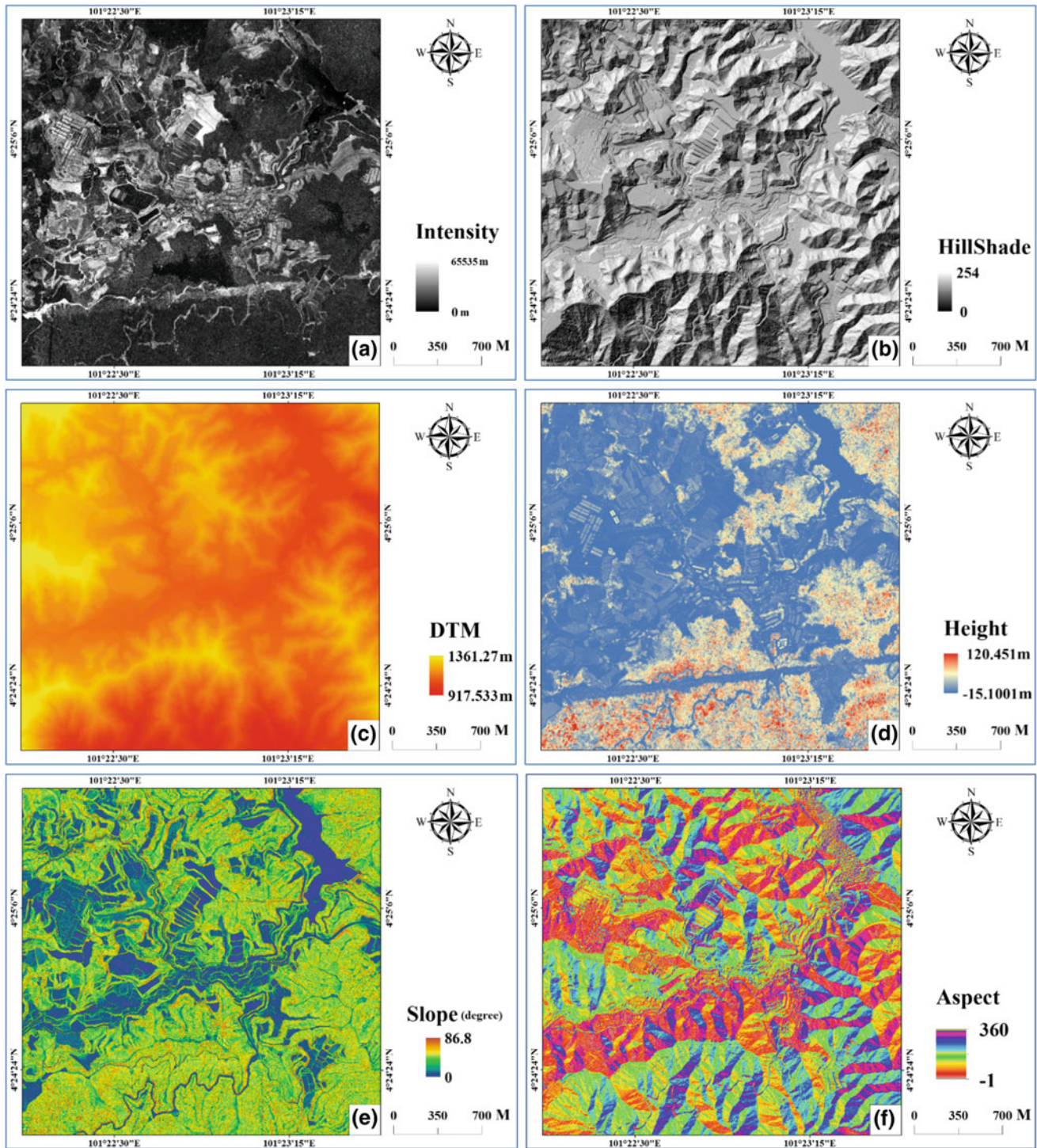


Fig. 3.5 LiDAR-derived data used for identification the location and direction of landslide include **a** intensity; **b** hillshade; **c** DTM; **d** height; **e** slope; and **f** aspect

as traditional pixel-based (Pradhan et al. 2016). The results of an object-based approach are more accurate (Rau et al. 2014) than pixel-based classification (Tehrany et al. 2014). As one of the most significant classification schemes, OBIA can provide valuable information for landslide inventory

mapping (Guzzetti et al. 2012). It is considered suitable for landslide inventory mapping because its image segmentation and classification processes resemble human knowledge, and existing knowledge can be transferred into a machine algorithm in the form of rule sets, which have been implemented

in landslide mapping (Barlow et al. 2003; Pradhan et al. 2016; Stumpf and Kerle 2011).

Image segmentation is the first step of OBIA (Pradhan et al. 2016). In this step, homogeneous pixels are grouped into non-overlapping regions based on spectral and geometric characteristics (Pal and Pal 1993). Multiresolution segmentation is a common algorithm that has been utilized in various earth science studies (Blaschke 2010). Numerous features of the objects can be used in multiresolution segmentation. In the current study, three parameters, namely scale, shape, and compactness, are selected for the analysis (Pradhan et al. 2016). Determining these parameters using the traditional trial-and-error method is a time-consuming and work-intensive procedure (Pradhan et al. 2016). Therefore, automatic and semiautomatic methods have been used to identify the optimal parameters in various studies (Anders et al. 2011; Belgiu and Drăguț 2014; Drăguț et al. 2010). Among the advanced methods for automatically selecting segmentation parameters are the Taguchi optimization technique proposed by and the fuzzy logic supervised approach presented by (Zhang et al. 2010). Therefore, automatic methods that utilize optimization algorithms (Pradhan et al. 2016) can best reduce the time required for selecting the segmentation parameters.

The selection of a small (possibly the minimum) feature set yields the best possible classification results, which is desirable for practical reasons (Kursa and Rudnicki 2010). Therefore, significant attributes should be selected to enhance the results of landslide detection in a certain area (Kursa and Rudnicki 2010). The selection of important (or relevant) attributes can help differentiate between landslide and non-landslide areas as well as better classify landslides according to their types (Van Westen et al. 2008). Several studies have used multiple attribute integration for landslide detection (Borghuis et al. 2007; Danneels et al. 2007; Hervás and Rosin 1996; Tapas R Martha, Kerle, Jetten, van Westen, & Kumar, 2010; Tapas Ranjan Martha et al. 2011; Moine et al. 2009; Stumpf and Kerle 2011). Chen et al. (2014) used 10 attributes for landslide identification; their results showed that the selected relevant attributes provided valuable information for landslide identification. The current study primarily aims to optimize the parameters of segmentation and the attributes for developing transferable rule sets for landslide detection and their characteristics by using high-resolution LiDAR data.

3.4.3 Image Segmentation

Image segmentation, which is a fundamental step of OBIA, is realized using both spatial and spectral information (Darwish et al. 2003). Segmenting the presented object by delineating their boundaries directly affects the quality and

performance of the classification process. Various segmentation algorithms have been previously elaborated and applied to remote sensing data sets (Dey et al. 2010). The purpose of these algorithms is to determine relatively homogenous and powerful segments. In the current study, the image segmentation process was implemented by first identifying the three main parameters. These parameters control the segmentation results and affect the classification process (Möller et al. 2007; Tian and Chen 2007). A supervised fuzzy logic approach was used to select the optimal parameters because the traditional method for identifying the aforementioned parameters is time-consuming.

3.4.4 Correlation-Based Feature Selection

Selecting only the relevant attributes enhances the quality of landslide identification and classification in a particular area (Kursa and Rudnicki 2010). Working with a large number of attributes generates several problems. First, the algorithms are slowed down because numerous resources have to be considered (Kursa and Rudnicki 2010). Second, a higher number of attributes than the number of observations result in low accuracy (Kohavi and John 1997). Third, irrelevant input features may lead to overfitting (Chen et al. 2014). Therefore, important attributes should be selected to improve the accuracy of the feature extraction results. In the current study, CFS was performed using Weka 3.7 software to select the relevant attributes. The method established by (Li et al. 2016) was adopted in this study. The CFS algorithm was applied to all the LiDAR-derived data and the additional texture and geometric features. CFS was performed to determine the feature subsets to be used for developing the rules for landslide identification and characterization. The CFS method has two basic steps: ranking the initial attributes and eliminating the least important attributes through an iterative process.

3.4.5 DT Classifiers

DT methods are data mining techniques that generate a graphical illustration of the feature classification process (Daniel 2014). In OBIA, the most important phase is the construction of the image interpretation model (knowledge) for the segmented objects. However, executing OBIA with other classifiers that are considered “black boxes” may be difficult; by contrast, DT classifiers are like “white boxes”; that is, users can easily interpret the links between the variables of different classes and the explanatory variables of remote sensing data (Li et al. 2016). The model generated via a DT method can be either a predictive or a descriptive model. Basically, establishing DT classifiers does not require the elaborate setting of

the domain knowledge or attribute; consequently, it has become popular for exploratory knowledge discovery. This type of method can provide a rapid and powerful mode of showing the structures of a data set and handle a high-dimensional data set. In the current study, a DT algorithm was used to generate the rule sets for landslide identification and characterization using CFS-derived attributes.

3.4.6 Landslide Mapping

An object-based classification method using a DT algorithm was used to produce a landslide inventory map for the study area. In this method, training data were required. Landslide training samples were collected from the orthophotos of the locations where landslides were identified via visual interpretation. The image objects were then classified using the DT algorithm, and rule sets were generated for landslides, non-landslide features, and the two types of landslides (i.e., shallow and deep-seated). The important features, namely mean slope, area, mean intensity, and gray level co-occurrence matrix (GLCM) homogeneity, were selected using the CFS method in Weka 3.7 software. Furthermore, classification was executed using the J48 algorithm in Weka 3.7. Consequently, rule sets were developed to differentiate landslides from non-landslide features, such as vegetation, building, bare soil, and man-made slopes. In addition, other rule sets were developed to distinguish the two types of landslides. The classification results were validated using the ROC method and through field investigations.

3.5 Results

3.5.1 Segmentation Parameters Selected Using a Fuzzy Logic Supervised Approach

The optimal segmentation parameters (i.e., scale, shape, and compactness) were selected using the fuzzy logic supervised approach developed by (Zhang et al. 2010). The best values of the segmentation parameters were determined based on an adequate number of training samples, which included shallow and deep-seated landslides. Table 3.1 shows the selected values for the three parameters. For example, the initial segmentation parameter values inputted into the fuzzy-based

optimization tool were 20, 0.3, and 0.1 for scale, shape, and compactness, respectively, as shown in (Fig. 3.6a). From these initial values and after 100 iterations, the best values for scale, shape, and compactness derived from the optimization tool were 46.37, 0.37, and 0.401, respectively.

3.5.2 Attributes Selected Using the CFS Approach

The use of a large number of attributes can decrease the accuracy of landslide detection because of the presence of irrelevant attributes. Therefore, significant attributes were selected using the CFS method. Table 3.2 shows the 10 attributes selected out of the initial 35 attributes, including spatial, texture, geometric, and LiDAR derivatives. As shown in Table 3.2, the most important attribute is the mean intensity of LiDAR data, followed by the mean digital terrain model DTM or altitude. Texture attributes, such as the gray level difference vector contrast, GLCM homogeneity, and GLCM StdDev, were also significant in detecting landslides and determining their types using LiDAR data. In addition, area, height, and GLCM standard were the last three important attributes.

3.5.3 Rule Sets Developed for Landslide Detection and Characterization

Rules sets were developed using the DT algorithm, and the optimized attributes were selected via CFS. In general, six sets of rules were established for extracting various features or land cover types, including vegetation, bare soil, cut slope, building, and landslide. The rules developed for landslide identification included mean slope, area, mean intensity, and GLCM homogeneity. The thresholds for these attributes are provided in Table 3.3. Figure 3.7 illustrated the results of rule set based on analysis area. For example, the selected threshold for the mean slope attribute is 28°. This result indicates that most of the landslides in the study area fall from a relatively highly sloped area, and the chance of landslides occurring in flat terrain areas is minimal. The rules developed for identifying cut slopes included attributes such as mean height, GLCM StdDev, and area of objects. On the basis of the rules developed for landslide and cut slope

Table 3.1 Segmentation parameters

Initial parameters				Iteration (optimal parameters)		
No.	Scale	Shape	Compactness	Scale	Shape	Compactness
1	20	0.3	0.1	46.37	0.37	0.401
2	50	0.1	0.1	73.52	0.52	0.5
3	80	0.1	0.1	100.33	0.65	0.65

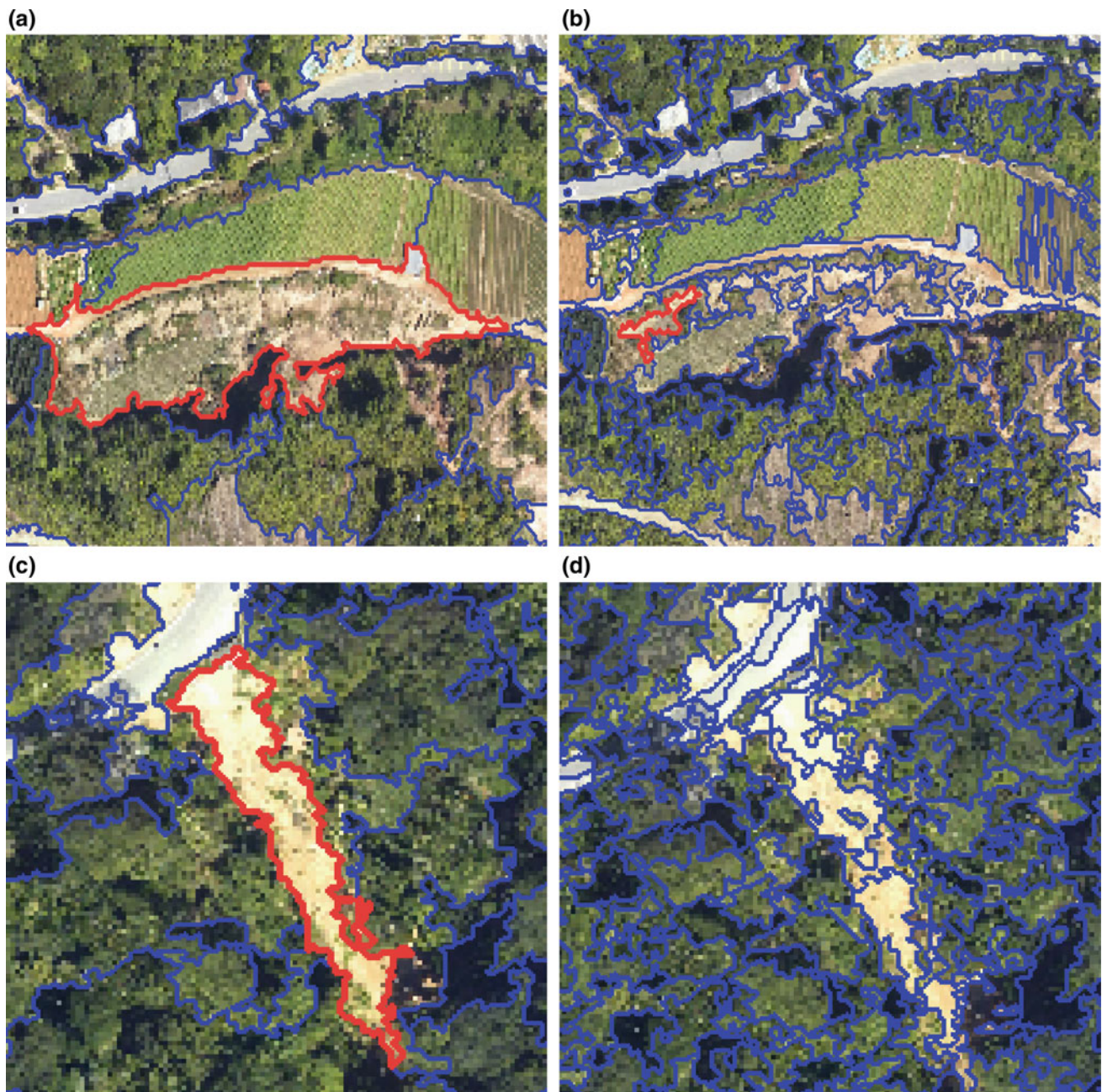


Fig. 3.6 **a** Initial segmentation for training site; **b** optimal segmentation for training site; **c** initial segmentation for test site; and **d** optimal segmentation for test site

detection, intensity and texture attributes (i.e., GLCM StdDev and GLCM homogeneity) are the most important attributes to differentiate the two land cover types.

The deep-seated landslides (10) in the study area are less than the shallow landslides (29). The detection accuracy for deep-seated landslides is higher than that for shallow landslides. (Lin et al. 2013) demonstrated that LiDAR data could significantly aid in identifying deep-seated landslides, particularly for densely vegetated areas. This current study showed that texture and LiDAR intensity attributes were

more significant for distinguishing between the two landslide types than other attributes. Table 3.4 shows that GLCM homogeneity and mean intensity attributes can effectively differentiate shallow from deep-seated landslides.

3.5.4 Model Transferability

In hilly and densely vegetated terrains, such as the Cameron Highlands, discriminating between landslides and man-made

Table 3.2 Outcomes of the attributes selection for landslide detection

Attribute	No. times	Rank
Mean intensity	20	1
Mean DTM	20	2
GLDV contrast	20	3
GLCM homogeneity	20	4
GLCM StdDev	20	6
Mean slope	20	7
Area	20	8
Height	20	9
GLCM standard	20	10

Table 3.3 Rules defined for landslide identification from non-landslide

Features	Rules define	Attributes
Vegetation	5.1 < Mean slope > 1.3 Area > 2837	LiDAR derivatives Spatial
Bare soil	GLCM standard <= 26.6 Area <= 4905	Spatial Spatial
Cut slope	Mean height <= 113.8 GLCM StdDev > 30.3 Area <= 2837	LiDAR derivatives Spatial Spatial
Building	Mean slope > 2.3 Mean height > 113.8	LiDAR derivatives LiDAR derivatives
Landslide	Mean slope > 28.0748 Area > 4905 Mean intensity <= 255.49 GLCM homogenous > = 0.0496	LiDAR derivatives Spatial LiDAR derivatives Spatial

slopes and distinguishing between the two types of landslides are challenging. Consequently, the results of transferability of the developed rule sets from analysis area to the entire area were tested as shown in Fig. 3.8. Two types of landslides were differentiated, namely shallow and deep-seated, by developed new rule set see Table 3.4. The results are shown in Fig. 3.9. Stumpf et al. (2011) said that the overall accuracy of landslide detection applied to other areas even if the same method was used for model development would frequently decrease. This decline in accuracy is ascribed to various reasons, including differences in landslide characteristics and environmental conditions. Differences in the sensors used, spatial resolutions of images, and illumination conditions are among the other challenges mentioned in a recent study (Rau et al. 2014).

3.6 Discussion

The identification of landslides and their types in densely vegetated areas, such as the Cameron Highlands, is challenging because of several reasons, including the presence of man-made slopes, dense vegetation, and hilly areas. This study presented a method for automatically detecting landslides and their types by using high-resolution LiDAR data.

The quantitative results of landslide identification demonstrated the robustness of the method. In addition, this study showed that optimizing the segmentation parameters, namely scale, shape, and compactness, by using the fuzzy logic supervised approach was satisfactory for differentiating non-landslide (i.e., vegetation and cut slope) from landslide features and between the two landslide types. Creating accurate objects through the optimized segmentation process allowed the use of spatial, texture, and geometric attributes for feature identification. Accurate segmentation is necessary to distinguish deep-seated from shallow landslides because landslides can be classified according to their geometric and texture attributes (Table 3.4).

The selection of the optimal attributes, which are relevant to a landslide, mainly relies on the experience of the analysts. Thus, establishing an attribute selection method is imperative to detect landslides and their characteristics. The relevant attributes selected using the CFS algorithm simplify the rule sets used to detect landslides and their types. In addition, the rules developed with less optimized attributes can be transferable to the entire study area. The optimized attributes for detecting landslides and determining their types included LiDAR-derived data (i.e., slope, height, and intensity), texture attributes (i.e., GLCM StdDev and GLCM homogeneity), and geometric attributes. Computation time and reliance

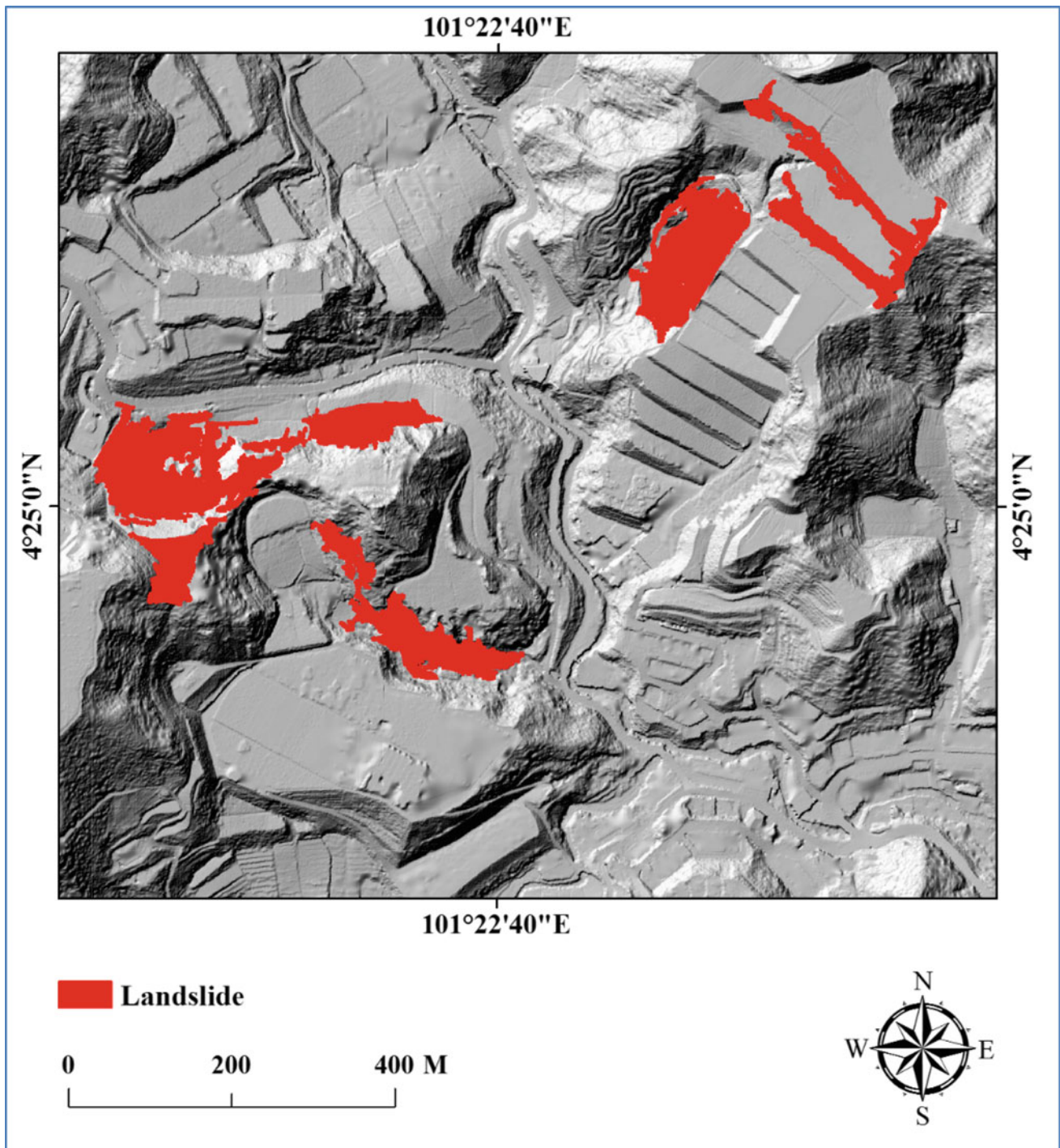


Fig. 3.7 Analysis area for detecting the location of landslide

Table 3.4 Rules defined to differentiate between types of landslide

Feature types	Rules define	Attributes
Deep-seated	GLCM homogenous ≤ 0.05	Spatial
	GLCM homogenous (Direction = 0°) > 0.038	Spatial
Shallow	GLCM homogenous > 0.05	Spatial
	Mean intensity ≤ 414.3	LiDAR derivatives
	GLCM homogenous (Direction = 0°) ≤ 0.038	Spatial

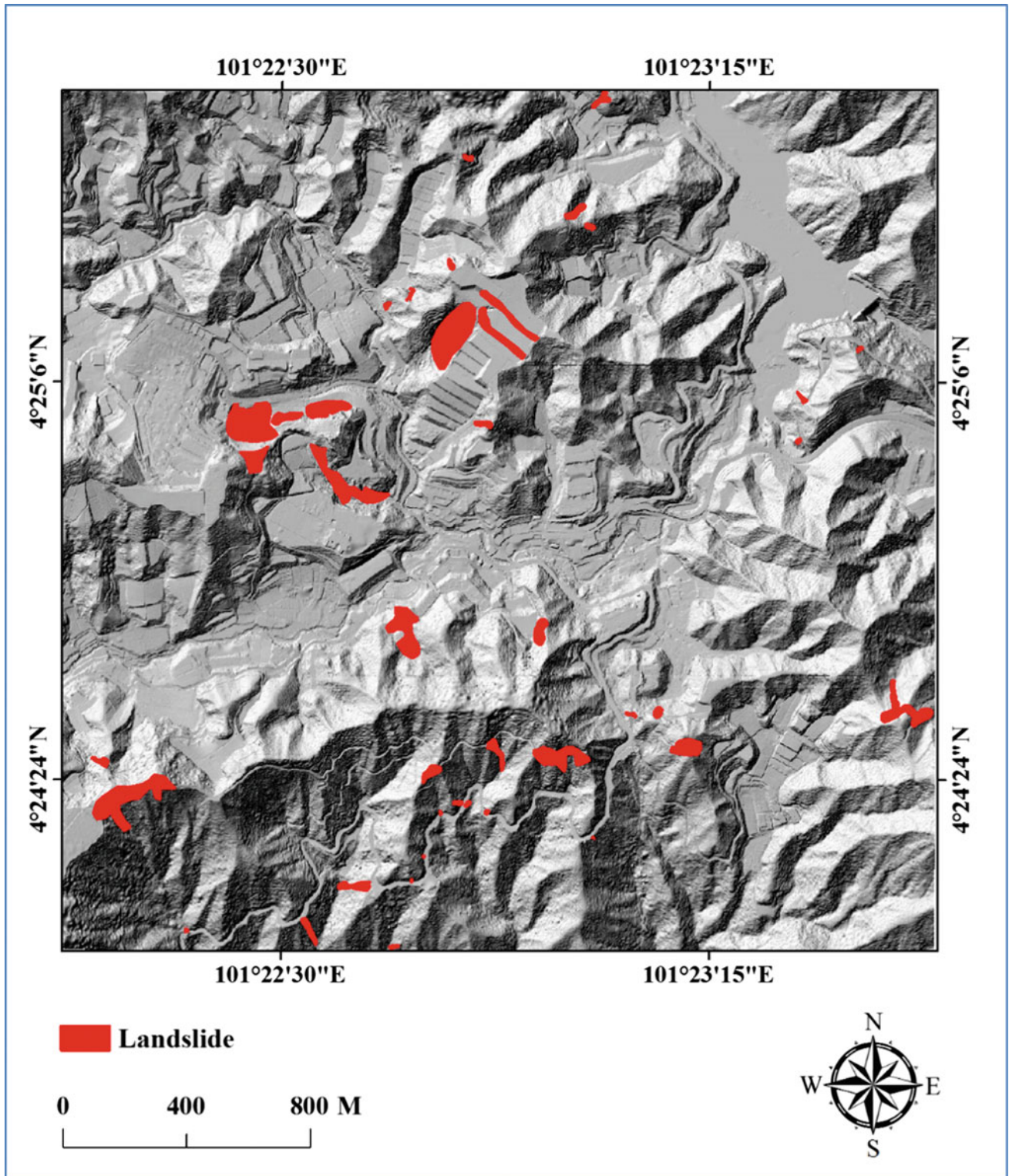


Fig. 3.8 Test area showing the locations of landslide in whole study area after transferability

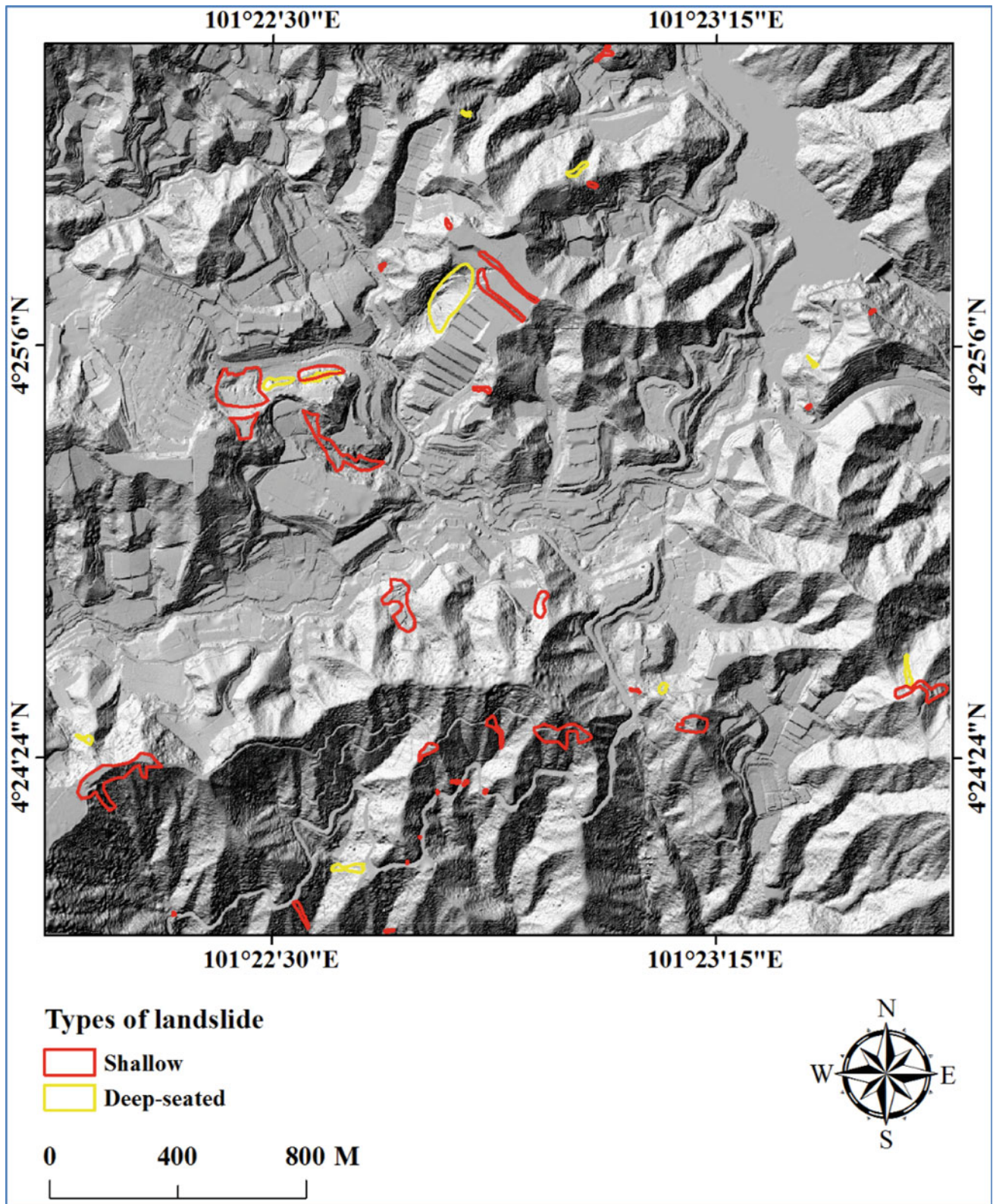


Fig. 3.9 Location of the shallow and deep-seated landslides in the study area

on the expert knowledge of the analyst were reduced to a greater extent with the proposed rule sets than with existing complex rule sets based on image classification.

Field investigation is challenging and tedious for mapping landslide inventories (Dou et al. 2015). Although the visual interpretation of remote sensing data using this method is reliable, this method is both costly and time-consuming. A new landslide detection method, which utilizes LiDAR-derived data, is effective for mapping geomorphic features and landslides, particularly in densely vegetated areas. The natural features of the earth surface are difficult to recognize using traditional methods (Chen et al. 2015). By contrast, a LiDAR-derived DEM provides additional terrain data, such as curvature, slope, and hillshade, which can help better describe the landscape of an area and identify landslides and their types. The current study used a LiDAR-derived DEM, as well as texture and geometric features, for landslide detection and characterization. The results show that LiDAR data can be effectively used to analyze and visualize terrains that are difficult to explore

because of the presence of dense vegetation. Furthermore, the locations of landslides were identified using the proposed method, and their directions were visualized by overlaying the slope and aspect factors from the LiDAR-derived data. The landslides were also rendered in 3D to visualize their other characteristics, such as width, length, runoff distance, and depth as shown in Fig. 3.10.

3.6.1 Accuracy Assessment

Various methods and accuracy metrics, such as kappa indices, overall accuracy, user's accuracy, and producer's accuracy, have been applied to estimate the accuracy of remote sensing products (Dou et al. 2015). The concept of a confusion matrix is frequently adopted to simplify the calculation of these accuracy metrics (Radoux and Bogaert 2014). In recent studies, however, the use of kappa indices has been criticized by several researchers (Pontius and Millones 2011). Mondini et al. (2011) utilized ROC plots to

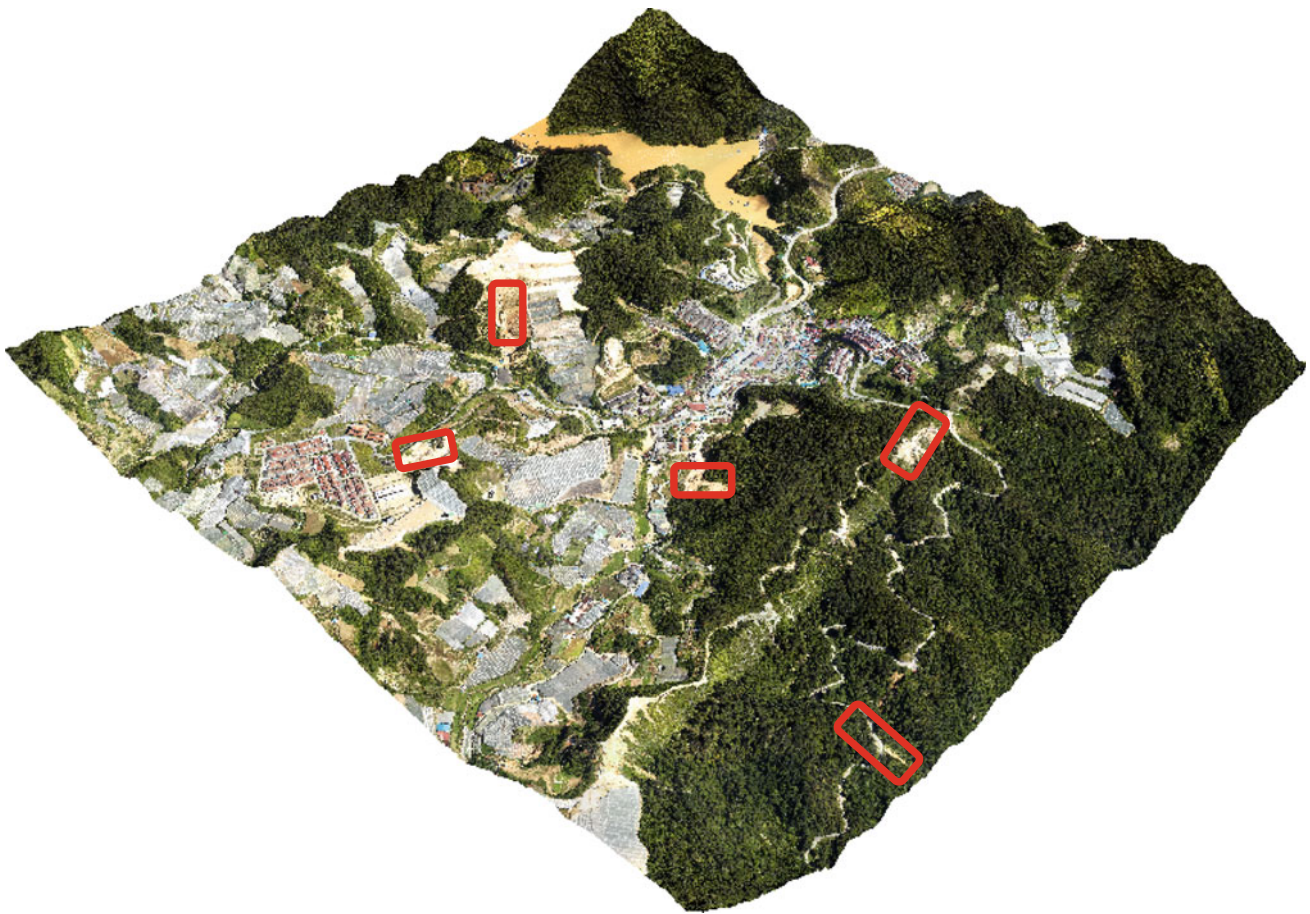


Fig. 3.10 3D perspective of detected landslides for the study area

evaluate remote sensing outcomes by plotting the true positive value against the positive predictive value (PPV). ROC plotting is one of the common methods used in engineering and signal processing; therefore, the use of this method to evaluate the quality of deterministic and probabilistic detection and forecast systems is extremely helpful. In the current study, the landslide detection results were assessed using the ROC plotting method and further verified through field investigations. The accuracy assessment is performed as follows: The locations of the landslides were first collected from the study area using a handheld Global Positioning System (GPS) device with an accuracy of 5 m. Subsequently, the ROC curves for shallow and deep-seated landslides were generated, and the AUCs were calculated. Figure 3.10 shows the ROC curves for landslide detection and their types as detected by the method proposed in the current study. The estimated AUC of landslide detection was 0.82, and the accuracy rates after transferability for shallow and deep-seated landslides were 0.80 and 0.83, respectively.

The estimated accuracy rates indicated the effectiveness of the proposed approach for detecting landslides and distinguishing their types (Fig. 3.11).

3.6.2 Field Investigation

A field investigation was conducted as an additional assessment method to examine the reliability of the proposed method. A handheld GPS device (GeoExplorer 6000) was used to identify the locations of the landslides, as shown in Fig. 3.12. The information acquired from field measurements allowed for the assessment of the precision and reliability of the produced landslide inventory map. In addition, the field investigation demonstrated that the landslides detected using the proposed methodology were accurate. Thus, the current methodology can identify landslide locations, distinguish landslide types, and produce a reasonable acceptable landslide inventory map for the Cameron Highlands.

Fig. 3.11 ROC curve for **a** detected landslides and their characteristics; **b** shallow landslide; and **c** deep-seated

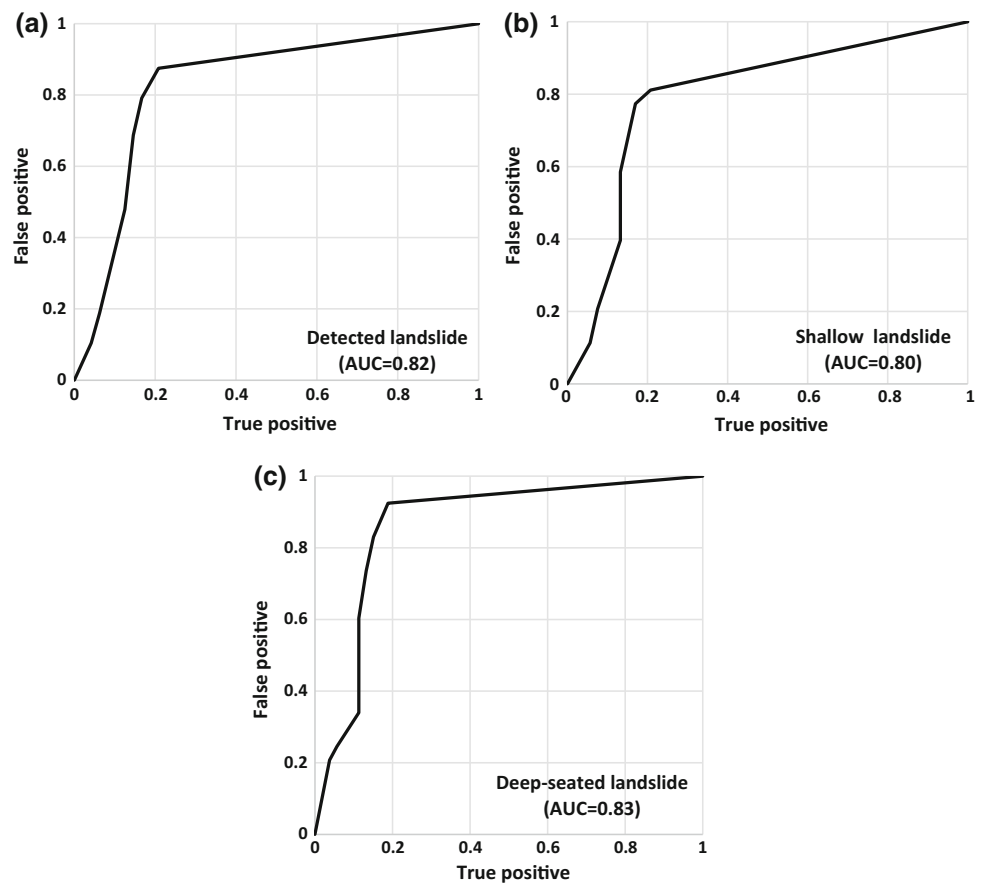




Fig. 3.12 Field photographs taken in the study area during field investigation

3.7 Conclusion

Identifying landslides and their types (i.e., shallow and deep-seated) in tropical regions is a difficult task. In this study, an optimized object-oriented rule set was developed to detect landslides in the Cameron Highlands and differentiate between their types. The main data sources were high-resolution airborne LiDAR point clouds. Optimized segmentation was performed using an existing fuzzy logic supervised approach, and the important attribute subset was selected using the CFS algorithm. The overall accuracy of landslide detection using the proposed method was 0.82, and the prediction accuracy rates for shallow and deep-seated landslide detection were 0.80 and 0.83, respectively. The optimization of the segmentation parameters and attributes improved the computational efficiency of the workflow and enhanced the transferability of the rule sets into different spatial subsets within the Cameron Highlands. LiDAR data were effective and useful for identifying landslides and distinguishing their types. In addition, the use of LiDAR data allowed for the identification of other characteristics of landslides, such as orientation and runoff distance, by

overlaying LiDAR-derived slope and aspect factors on detected landslide scarps. The optimization of segmentation parameters and the selection of attributes could also improve the computational efficiency of the workflow and enhance the transferability of the rule sets into different spatial subsets within the Cameron Highlands in Malaysia. This study suggests that developing rule sets based on optimized techniques and using VHR airborne LiDAR-derived data and spatial attributes are effective in identifying the locations of landslides and distinguishing their types in tropical regions. This proposed automatic landslide detection method can be an important geospatial solution for managing landslide hazards and conducting landslide risk assessments.

References

- Agliardi, F., Crosta, G. B., Zanchi, A., & Ravazzi, C. (2009). Onset and timing of deep-seated gravitational slope deformations in the eastern Alps, Italy. *Geomorphology*, 103(1), 113–129.
- Anders, N. S., Seijmonsbergen, A. C., & Bouten, W. (2011). Segmentation optimization and stratified object-based analysis for

- semi-automated geomorphological mapping. *Remote Sensing of Environment*, 115(12), 2976–2985.
- Bai, S., Wang, J., Zhang, Z., & Cheng, C. (2012). Combined landslide susceptibility mapping after Wenchuan earthquake at the Zhouqu segment in the Bailongjiang Basin, China. *Catena*, 99, 18–25.
- Barlow, J., Martin, Y., & Franklin, S. (2003). Detecting translational landslide scars using segmentation of Landsat ETM+ and DEM data in the northern Cascade Mountains, British Columbia. *Canadian Journal of Remote Sensing*, 29(4), 510–517.
- Belgiu, M., & Drăguț, L. (2014). Comparing supervised and unsupervised multiresolution segmentation approaches for extracting buildings from very high resolution imagery. *ISPRS Journal of Photogrammetry and Remote Sensing*, 96, 67–75.
- Blaschke, T. (2010). Object based image analysis for remote sensing. *ISPRS Journal of Photogrammetry and Remote Sensing*, 65(1), 2–16.
- Borghuis, A., Chang, K., & Lee, H. (2007). Comparison between automated and manual mapping of typhoon-triggered landslides from SPOT-5 imagery. *International Journal of Remote Sensing*, 28(8), 1843–1856.
- Brunetti, M., Guzzetti, F., & Rossi, M. (2009). Probability distributions of landslide volumes. *Nonlinear Processes in Geophysics*, 16(2), 179–188.
- Bugnion, L., Volkwein, A., & Denk, M. (2009). *Artificial full scale shallow landslides*. Paper presented at the EGU General Assembly Conference Abstracts.
- Chang, K.-T., Liu, J.-K., & Wang, C.-I. (2012). An object-oriented analysis for characterizing the rainfall-induced shallow landslide. *Journal of Marine Science and Technology*, 20(6), 647–656.
- Chen, R.-F., Lin, C.-W., Chen, Y.-H., He, T.-C., & Fei, L.-Y. (2015). Detecting and characterizing active thrust fault and deep-seated landslides in dense forest areas of Southern Taiwan Using Airborne LiDAR DEM. *Remote Sensing*, 7(11), 15443–15466.
- Chen, W., Li, X., Wang, Y., Chen, G., & Liu, S. (2014). Forested landslide detection using LiDAR data and the random forest algorithm: A case study of the Three Gorges, China. *Remote Sensing of Environment*, 152, 291–301.
- Cruden, D. M., & Varnes, D. J. (1996). Landslides: investigation and mitigation. Chapter 3-Landslide types and processes. *Transportation research board special report* (247).
- Daniel, S. (2014). *Predictive modeling of trust to Social Media content*.
- Danneels, G., Pirard, E., & Havenith, H.-B. (2007). *Automatic landslide detection from remote sensing images using supervised classification methods*. Paper presented at the 2007 IEEE International Geoscience and Remote Sensing Symposium.
- Darwish, A., Leukert, K., & Reinhardt, W. (2003). *Image segmentation for the purpose of object-based classification*. Paper presented at the International Geoscience and Remote Sensing Symposium.
- Delgado, J., Vicente, F., García-Tortosa, F., Alfaro, P., Estévez, A., Lopez-Sanchez, J., et al. (2011). A deep seated compound rotational rock slide and rock spread in SE Spain: Structural control and DInSAR monitoring. *Geomorphology*, 129(3), 252–262.
- Dey, V., Zhang, Y., & Zhong, M. (2010). *A review on image segmentation techniques with remote sensing perspective*: na.
- eDomlija, P., Bernat, S., Mihalić, S. A., & Benac, Č. (2014). Landslide inventory in the area of Dubračina River Basin (Croatia) *Landslide science for a safer geoenvironment* (pp. 837–842). Berlin: Springer.
- Dou, J., Chang, K.-T., Chen, S., Yunus, A. P., Liu, J.-K., Xia, H., et al. (2015a). Automatic case-based reasoning approach for landslide detection: Integration of object-oriented image analysis and a genetic algorithm. *Remote Sensing*, 7(4), 4318–4342.
- Dou, J., Paudel, U., Oguchi, T., Uchiyama, S., & Hayakavva, Y. S. (2015). Shallow and deep-seated landslide differentiation using support vector machines: A case study of the Chuetsu Area, Japan. *Terrestrial, Atmospheric & Oceanic Sciences*, 26(2).
- Drăguț, L., Tiede, D., & Levick, S. R. (2010). ESP: A tool to estimate scale parameter for multiresolution image segmentation of remotely sensed data. *International Journal of Geographical Information Science*, 24(6), 859–871.
- Gao, J., & Maro, J. (2010). Topographic controls on evolution of shallow landslides in pastoral Wairarapa, New Zealand, 1979–2003. *Geomorphology*, 114(3), 373–381.
- Goudie, A. (2004). *Encyclopedia of geomorphology* (Vol. 2). UK: Psychology Press.
- Guzzetti, F., Mondini, A. C., Cardinali, M., Fiorucci, F., Santangelo, M., & Chang, K.-T. (2012). Landslide inventory maps: New tools for an old problem. *Earth-Science Reviews*, 112(1), 42–66.
- Heleno, S., Matias, M., Pina, P., & Sousa, A. (2015). Automated object-based classification of rain-induced landslides with VHR multispectral images in Madeira Island. *Natural Hazards & Earth System Sciences Discussions*, 3(9).
- Hervás, J., & Rosin, P. L. (1996). *Landslide mapping by textural analysis of ATM data*. Paper presented at the Proceedings of the Thematic Conference on Geologic Remote Sensing.
- Hong, Y., He, X., Cerato, A., Zhang, K., Hong, Z., & Liao, Z. (2015). Predictability of a physically based model for rainfall-induced shallow landslides: Model development and case studies. In *Modern technologies for landslide monitoring and prediction* (pp. 165–178). New York: Springer.
- Kasai, M., Ikeda, M., Asahina, T., & Fujisawa, K. (2009). LiDAR-derived DEM evaluation of deep-seated landslides in a steep and rocky region of Japan. *Geomorphology*, 113(1), 57–69.
- Kellerer-Pirklbauer, A., Proske, H., & Strasser, V. (2010). Paraglacial slope adjustment since the end of the Last Glacial Maximum and its long-lasting effects on secondary mass wasting processes: Hauser Kaibling, Austria. *Geomorphology*, 120(1), 65–76.
- Kohavi, R., & John, G. H. (1997). Wrappers for feature subset selection. *Artificial Intelligence*, 97(1), 273–324.
- Korup, O. (2006). Effects of large deep-seated landslides on hillslope morphology, western Southern Alps, New Zealand. *Journal of Geophysical Research: Earth Surface*, 111(F1).
- Kursa, M. B., & Rudnicki, W. R. (2010). Feature selection with the Boruta package: Journal.
- Li, M., Ma, L., Blaschke, T., Cheng, L., & Tiede, D. (2016). A systematic comparison of different object-based classification techniques using high spatial resolution imagery in agricultural environments. *International Journal of Applied Earth Observation and Geoinformation*, 49, 87–98.
- Lin, C.-W., Tseng, C.-M., Tseng, Y.-H., Fei, L.-Y., Hsieh, Y.-C., & Tarolli, P. (2013). Recognition of large scale deep-seated landslides in forest areas of Taiwan using high resolution topography. *Journal of Asian Earth Sciences*, 62, 389–400.
- Ma, H.-R., Cheng, X., Chen, L., Zhang, H., & Xiong, H. (2016). Automatic identification of shallow landslides based on World-view2 remote sensing images. *Journal of Applied Remote Sensing*, 10(1), 016008.
- Malamud, B. D., Turcotte, D. L., Guzzetti, F., & Reichenbach, P. (2004). Landslide inventories and their statistical properties. *Earth Surface Processes and Landforms*, 29(6), 687–711.
- Martha, T. R., Kerle, N., Jetten, V., van Westen, C. J., & Kumar, K. V. (2010). Characterising spectral, spatial and morphometric properties of landslides for semi-automatic detection using object-oriented methods. *Geomorphology*, 116(1), 24–36.
- Martha, T. R., Kerle, N., van Westen, C. J., Jetten, V., & Kumar, K. V. (2011). Segment optimization and data-driven thresholding for knowledge-based landslide detection by object-based image analysis. *IEEE Transactions on Geoscience and Remote Sensing*, 49(12), 4928–4943.

- McKean, J., & Roering, J. (2004). Objective landslide detection and surface morphology mapping using high-resolution airborne laser altimetry. *Geomorphology*, 57(3), 331–351.
- Moine, M., Puissant, A., & Malet, J.-P. (2009). *Detection of landslides from aerial and satellite images with a semi-automatic method*. Application to the Barcelonnette basin (Alpes-de-Hautes-Provence, France): Paper presented at the Landslide processes-from geomorphologic mapping to dynamic modelling.
- Möller, M., Lymburner, L., & Volk, M. (2007). The comparison index: A tool for assessing the accuracy of image segmentation. *International Journal of Applied Earth Observation and Geoinformation*, 9(3), 311–321.
- Mondini, A., Guzzetti, F., Reichenbach, P., Rossi, M., Cardinali, M., & Ardizzone, F. (2011). Semi-automatic recognition and mapping of rainfall induced shallow landslides using optical satellite images. *Remote Sensing of Environment*, 115(7), 1743–1757.
- Pal, N. R., & Pal, S. K. (1993). A review on image segmentation techniques. *Pattern Recognition*, 26(9), 1277–1294.
- Pontius, R. G., Jr., & Millones, M. (2011). Death to Kappa: Birth of quantity disagreement and allocation disagreement for accuracy assessment. *International Journal of Remote Sensing*, 32(15), 4407–4429.
- Pradhan, B., Jebur, M. N., Shafri, H. Z. M., & Tehrany, M. S. (2016). Data fusion technique using wavelet transform and taguchi methods for automatic landslide detection from airborne laser scanning data and quickbird satellite imagery. *IEEE Transactions on Geoscience and Remote Sensing*, 54(3), 1610–1622.
- Radoux, J., & Bogaert, P. (2014). Accounting for the area of polygon sampling units for the prediction of primary accuracy assessment indices. *Remote Sensing of Environment*, 142, 9–19.
- Rau, J.-Y., Chang, K.-T., Shao, Y.-C., & Lau, C.-C. (2012). Semi-automatic shallow landslide detection by the integration of airborne imagery and laser scanning data. *Natural Hazards*, 61(2), 469–480.
- Rau, J.-Y., Jhan, J.-P., & Rau, R.-J. (2014). Semiautomatic object-oriented landslide recognition scheme from multisensor optical imagery and DEM. *IEEE Transactions on Geoscience and Remote Sensing*, 52(2), 1336–1349.
- Segoni, S., Leoni, L., Benedetti, A., Catani, F., Righini, G., Falorni, G., et al. (2009). Towards a definition of a real-time forecasting network for rainfall induced shallow landslides. *Natural Hazards and Earth System Sciences*, 9(6), 2119–2133.
- Stumpf, A., & Kerle, N. (2011). Object-oriented mapping of landslides using Random Forests. *Remote Sensing of Environment*, 115(10), 2564–2577.
- Stumpf, A., Lachiche, N., Malet, J.-P., Kerle, N., & Puissant, A. (2014). Active learning in the spatial domain for remote sensing image classification. *IEEE Transactions on Geoscience and Remote Sensing*, 52(5), 2492–2507.
- Tarolli, P. (2014). High-resolution topography for understanding Earth surface processes: Opportunities and challenges. *Geomorphology*, 216, 295–312.
- Tehrany, M. S., Pradhan, B., & Jebur, M. N. (2014). A comparative assessment between object and pixel-based classification approaches for land use/land cover mapping using SPOT 5 imagery. *Geocarto International*, 29(4), 351–369.
- Tian, J., & Chen, D. M. (2007). Optimization in multi-scale segmentation of high-resolution satellite images for artificial feature recognition. *International Journal of Remote Sensing*, 28(20), 4625–4644.
- van Asselen, S., & Seijmonsbergen, A. (2006). Expert-driven semi-automated geomorphological mapping for a mountainous area using a laser DTM. *Geomorphology*, 78(3), 309–320.
- Van Westen, C. J., Castellanos, E., & Kuriakose, S. L. (2008). Spatial data for landslide susceptibility, hazard, and vulnerability assessment: An overview. *Engineering Geology*, 102(3), 112–131.
- Vennari, C., Gariano, S., Antronico, L., Brunetti, M., Iovine, G., Peruccacci, S., et al. (2014). Rainfall thresholds for shallow landslide occurrence in Calabria, southern Italy. *Natural Hazards and Earth System Sciences*, 14(2), 317–330.
- Vohora, V., & Donoghue, S. (2004). *Application of remote sensing data to landslide mapping in Hong Kong*. Remote Sensing and Spatial Information Sciences: International Archives of Photogrammetry.
- Wiegand, C., Rutzinger, M., Heinrich, K., & Geitner, C. (2013). Automated extraction of shallow erosion areas based on multi-temporal ortho-imagery. *Remote Sensing*, 5(5), 2292–2307.
- Yu, T.-T., Wang, T.-S., & Cheng, Y.-S. (2015). Analysis of factors triggering shallow failure and deep-seated landslides induced by single rainfall events. *Journal of Disaster Research*, 10(5), 966–972.
- Zêzere, J. L., Trigo, R. M., & Trigo, I. F. (2005). Shallow and deep landslides induced by rainfall in the Lisbon region (Portugal): Assessment of relationships with the North Atlantic Oscillation. *Natural Hazards and Earth System Science*, 5(3), 331–344.
- Zhang, Y., Maxwell, T., Tong, H., & Dey, V. (2010). *Development of a supervised software tool for automated determination of optimal segmentation parameters for ecognition*: na.
- Zizioli, D., Meisina, C., Bordonni, M., & Zucca, F. (2014). Rainfall-triggered shallow landslides mapping through Pleiades images In *Landslide science for a safer geoenvironment* (pp. 325–329). New York: Springer.